Construction of Fully Conjugated Covalent Organic Frameworks via Facile Linkage Conversion for Efficient Photoenzymatic Catalysis

Yuancheng Wang,[†,+] Hui Liu,[†,+] Qingyan Pan,[†] Chenyu Wu,[†] Wenbo Hao,[†] Jie Xu,[†] Renzeng Chen,[†] Jian Liu,[‡] Zhibo Li,*[,†] and Yingjie Zhao*[,†]

[†]*Key Laboratory of Biobased Polymer Materials, Shandong Provincial Education Department; College of Polymer Science and Engineering, Qingdao University of Science and Technology, Qingdao 266042, China*

[‡]*College of Materials Science and Engineering, Qingdao University of Science and Technology, Qingdao 266042, China*

[*] Corresponding Authors: zbli@qust.edu.cn, yz@qust.edu.cn

[+] These authors contributed equally to this work.

Supporting Information

Table of Contents

1. Supporting Methods

1.1 General materials and methods

Unless otherwise specified, all reactions were performed in dried glassware under ambient atmosphere. All other reagents were purchased commercially and used without further purification. Organic solvents including ethanol, dichloromethane (DCM), petroleum ether, 2,2'-bipyridine, tris(2-hydroxy ethyl)amine (TEOA), triethanolamine dichloro(pentamethylcyclopenta-dienyl) rhodium(III) dimer, phosphate buffer, nicotinamide adenine dinucleotide (NAD^+), α-ketoglutarate, diammonium hydrogen phosphate, trifluoromethane sulfonic acid, trifluoroacetic acid and benzaldehyde were purchased from Adamas; 1,2-Dichlorobenzene, n-butanol and 1,4-dioxane were purchased from Alfa Aesar; dilute hydrochloric acid was purchased from Yantai Far East Fine Chemical Co., Ltd. All aqueous solutions were prepared with Milli-Q water.

^1H and ^{13}C NMR spectra were performed on 400 MHz spectrometers (Bruker AVANCE NEO 400 Ascend) in the indicated solvents at room temperature. High resolution solid-state NMR spectra were recorded on Agilent NMR Spectrometer (60054-ASC) using a standard CP pulse sequence probe with 4 mm (outside diameter) zirconia rotors. Mass spectra were recorded with Waters GCT high-resolution mass spectrometer.

Transmission electron microscope (TEM) were performed on a JEM-2100 electron microscope with an accelerating voltage of 200 kV.

TGA was carried out on an American TA-Q20 in nitrogen atmosphere using a 10 °C/min ramp without equilibration delay.

The liquid UV-Vis absorbance was measured by UV spectrophotometer (HITACHI, U-2910). The Solid-state UV-Vis absorbance were measured by UV spectrophotometer (HITACHI, U-3900).

Powder X-ray diffraction (PXRD) patterns were obtained on a PANalytical

Empyrean X-Ray diffractometer with Cu Kα line focused radiation at 40 kV and 40 mA from 2θ = 1.5° up to 40° with 0.02° increment by Bragg-Brentano. The powdered sample was added to the glass and compacted for measurement.

N_2 adsorption isotherms were measured up to 1 bar at 77 K using a Micrometrics ASAP 2460 surface area analyzer. Prior to measurements, samples (ca. 50 mg) were degassed for over 12 h at 120 °C. UHP grade N_2 and He were used throughout the adsorption experiments. Oil-free vacuum pumps and oil-free pressure regulators were used for measurements to prevent contamination of the samples during the degassing process and isotherm measurement.

Cyclic voltammetry (CV) was performed using a standard one compartment, three electrode electrochemical cell attached to an CHI 760E Electrochemical Workstation. The Ag/AgCl aqueous electrode was used as reference electrode. Glass-carbon was used as the working electrode, and Pt was used as the counter electrode. Tetrabutylammonium hexafluorophosphate (0.1 M) in acetonitrile was used as electrolyte.

***Photocatalytic NADH Production*:** Photo regeneration of NADH was irradiated with a xenon lamp (300 W) through a 420 nm cut off filter, avoiding the UV light-induced damage of the enzyme with a distance of 10 cm. The photocatalytic regeneration of NADH was carried out as follows. The reaction was performed in a quartz reactor. The reaction medium was composed of $[Cp^*Rh(bpy)(H)]^+$ (0.75 μmol), β-NAD^+ (3 μmol), TEOA (2.01 mmol), 600 μL of 4 M HCl solution and COF (3 mg) in 2.1 mL of phosphate buffer (100 mM, pH = 7.0). The reactor was initially allowed to equilibriate in dark for 30 minutes, following which it was exposed to visible light. The regeneration of NADH was monitored by UV-vis spectrophotometer (U-3900, HITACHI). NADH has peak absorption at 340 nm with an extinction coefficient of 6220 M^{-1} cm^{-1}. During the illumination, the concentration of NADH was estimated by measuring the absorbance of the diluted reaction system at 340 nm.

1.2 Synthesis procedure

1,3,5-tris(4-formylphenyl)-benzene and 2,4,6-tris(4-formylphenyl)-1,3,5-triazine were prepared according to the references.[S1-S2]

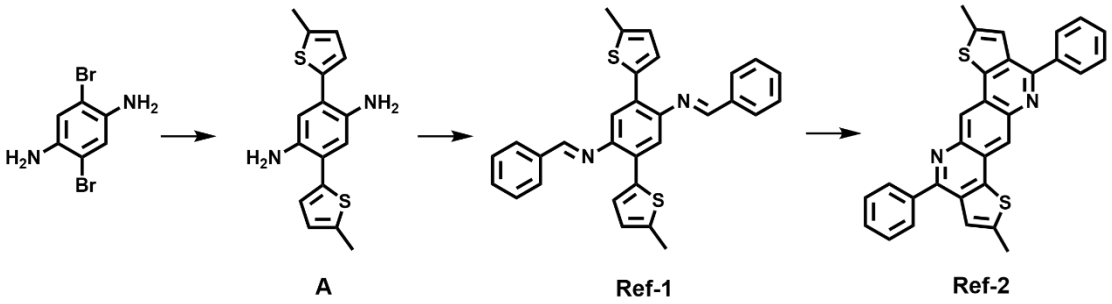

Synthesis of 2,5-bis(5-methylthiophen-2-yl)benzene-1,4-diamine (A).

A mixture of 2,5-dibromobenzene-1,4-diamine (1.00 g, 3.76 mmol), 4,4,5,5-Tetra methyl-2-(5-methyl-2-thienyl)-1,3,2-dioxaborolane (2.53 g, 11.28 mmol), $Pd_2(dba)_3$ (172.2 mg, 0.19 mmol) and Xphos (181.2 mg, 0.38 mmol) in the mixed solvent containing tetrahydrofuran (50 mL) and 2.0 M K_2CO_3 (aq) (15 mL) was refluxed at 80 °C under nitrogen overnight. After cooling down to room temperature, the mixture was extracted with ethyl acetate. The organic phase was dried with $MgSO_4$ and condensed under reduced pressure. The residue was purified by chromatography (SiO_2, 50% petroleum ether in dichloromethane) to give the product as light yellow solid powder (0.93 g, 82.1%). ^{1}H NMR (400 MHz, DMSO-d_6, δ): 7.04 (d, J = 3.5 Hz, 2H), 6.80 (dd, J_1 = 1.2 Hz, J_2 = 3.5 Hz, 2H), 6.73 (s, 2H), 4.41 (s, 4H), 2.46 (d, J = 1.1 Hz, 6H). ^{13}C NMR (100 MHz, DMSO-d_6, δ): 139.4, 138.6, 136.7, 126.5, 125.6, 120.5, 117.8, 15.4. HRMS (EI) m/z: [M^+] calcd. for $C_{16}H_{16}N_2S_2$ 300.0755; found 300.0753.

Synthesis of model compound Ref-1

To a 25 mL flask was added compound A (100 mg, 0.33 mmol), benzaldehyde (106.0 mg, 1.00 mmol), 5 mL ethanol and 1 mL chloroform. The mixture was refluxed overnight and then dropped into 20 mL cold ethanol. The precipitate was centrifuged and washed with ethanol and acetone before dried to obtain yellow solid (99% yield). ^{1}H NMR (400 MHz, $CDCl_2CDCl_2$, δ): 8.62 (s, 2H), 8.10 (dd, J_1 = 3.2 Hz, J_2 = 6.3 Hz

4H), 7.63 (t, J = 3.2 Hz, 6H), 7.42 (s, 2H), 7.39 (d, J = 3.6 Hz, 2H), 6.84 (dd, J_1 = 3.6 Hz, J_2 = 1.3 Hz, 2H), 2.58 (d, J = 1.0 Hz, 6H). ^{13}C NMR (100 MHz, $CDCl_2CDCl_2$, δ): 160.0, 146.2, 142.5, 137.7, 136.3, 131.8, 129.6, 129.2, 127.8, 126.3, 125.6, 117.3, 15.6. HRMS (EI) m/z: [M^+] calcd. for $C_{30}H_{24}N_2S_2$ 476.1381; found 476.1383.

Synthesis of model compound Ref-2

To a screw cap teflon-sealed tube was added **Ref-1** (100 mg, 0.21 mmol) and 4 mL dried toluene. After bubbling with oxygen for 10 min, 2 ml trifluoro acetic acid was added to the tube and then the tube was sealed. The reaction mixture was stirred at 100 ℃ for 24 h under oxygen atmosphere. After cooling to room temperature, the solvent was removed under vacuum and the crude product was recrystallized with dimethyl sulfoxide, filtered and washed with ethanol to obtain yellow crystal (88.2 mg, 89%). ^{1}H NMR (400 MHz, $CDCl_2CDCl_2$, δ): 8.87 (s, 2H), 7.89 (d, J = 7.0 Hz, 4H), 7.51-7.56 (m, 6H), 7.28 (s, 2H), 2.63 (s, 6H). ^{13}C NMR (100 MHz, $CDCl_2CDCl_2$, δ): 155.6, 145.2, 141.9, 141.6, 140.1, 132.4, 129.6, 129.5, 128.8, 124.1, 123.4, 123.4, 16.4. HRMS (EI) m/z: [M^+] calcd. for $C_{30}H_{20}N_2S_2$ 472.1068; found 472.1061.

Synthesis of B-COF-1.

By condensing compound A (35.0 mg, 0.116 mmol) and 1,3,5-tris(4-formylphenyl)-benzene (30.3 mg, 0.078 mmol) in the mixture of 1,2-dichlorobenzene/n-butanol/acetic acid (8:2:1, by volume) at 120 °C for 72 h, B-COF-1 was isolated as yellowish orange powder insoluble in common organic solvents (^{13}C CP/MAS spectra shown as Figure 1).

Synthesis of T-COF-1.

By condensing compound A (35.0 mg, 0.116 mmol) and 2,4,6-tris(4-formylphenyl)-1,3,5-triazine (30.6 mg, 0.078 mmol) in the mixture of 1,2-dichlorobenzene/n-butanol/acetic acid (8:2:1, by volume) at 120 °C for 72 h, B-COF-1 was isolated as orange red powder insoluble in common organic solvents (^{13}C CP/MAS spectra shown as Figure 1).

Synthesis of B-COF-2.

B-COF-1 (50 mg) and 3 mL dried toluene was added to a screw cap teflon-sealed tube. After bubbling with oxygen for 10 min, 2 ml trifluoro acetic acid was added to the tube and then the tube was sealed and heated at 100 ℃ for 2 days. B-COF-2 was isolated as yellow powder insoluble in common organic solvents (^{13}C CP/MAS spectra shown as Figure 1).

Synthesis of T-COF-2.

T-COF-1 (50 mg) and 3 mL dried toluene was added to a screw cap teflon-sealed tube. After bubbling with oxygen for 10 min, 2 ml trifluoro acetic acid was added to the tube and then the tube was sealed and heated at 100 ℃ for 2 days. T-COF-2 was isolated as yellow powder insoluble in common organic solvents (^{13}C CP/MAS spectra shown as Figure 1).

2. Supporting Figures and Legends

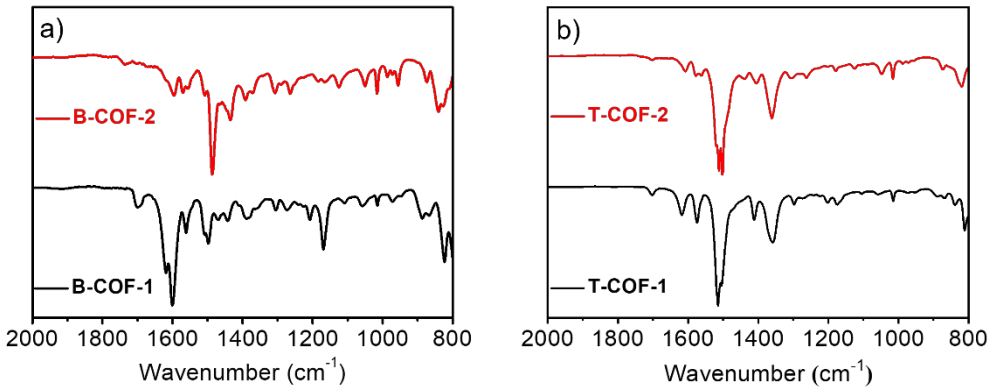

Figure S1. The FT-IR spectra of **B-COF-1, 2** (a) and **T-COF-1, 2** (b).

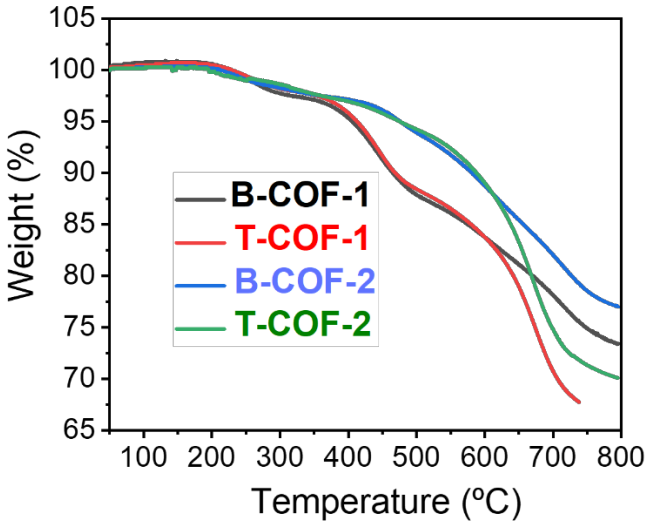

Figure S2. The thermogravimetric analysis profiles of **B-COF-1**, **2** and **T-COF-1**, **2**.

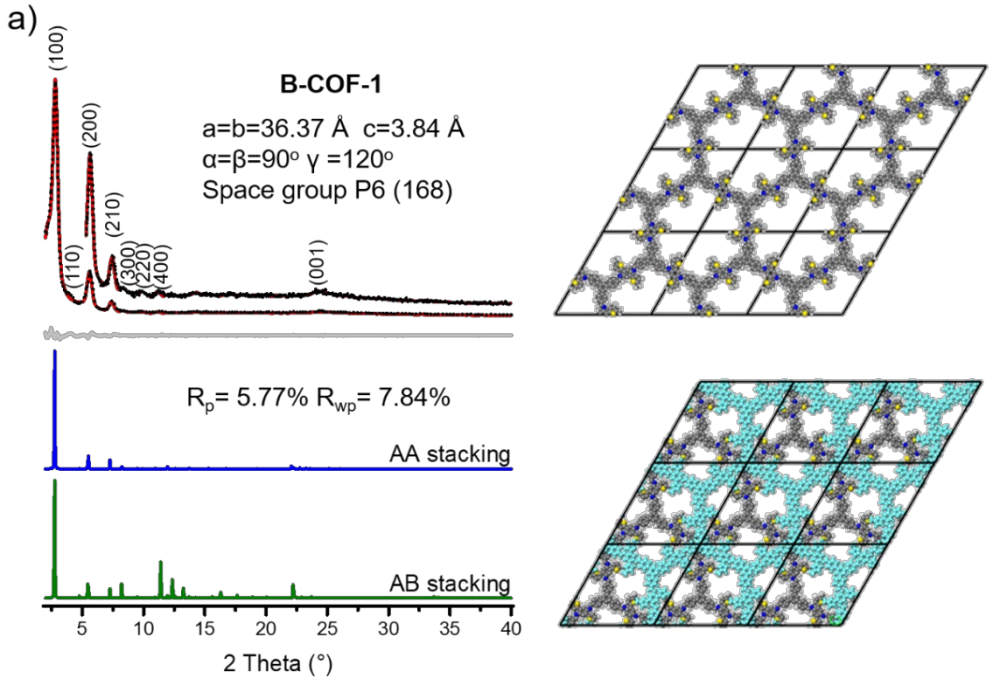
a)
B-COF-1
a=b=36.37 Å c=3.84 Å
α=β=90° γ =120°
Space group P6 (168)
(100)
(200)
(210)
(110)
(300)
(220)
(400)
(001)
R_p= 5.77% R_{wp}= 7.84%
AA stacking
AB stacking
5 10 15 20 25 30 35 40
2 Theta (°)

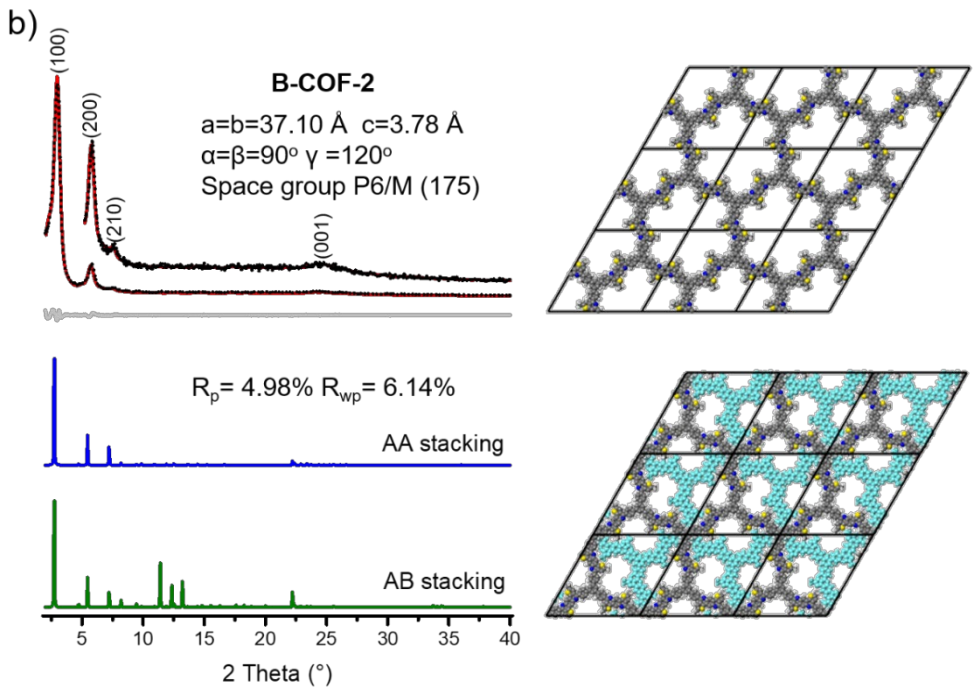
b)
B-COF-2
a=b=37.10 Å c=3.78 Å
α=β=90° γ =120°
Space group P6/M (175)
(100)
(200)
(210)
(001)
R_p= 4.98% R_{wp}= 6.14%
AA stacking
AB stacking
5 10 15 20 25 30 35 40
2 Theta (°)

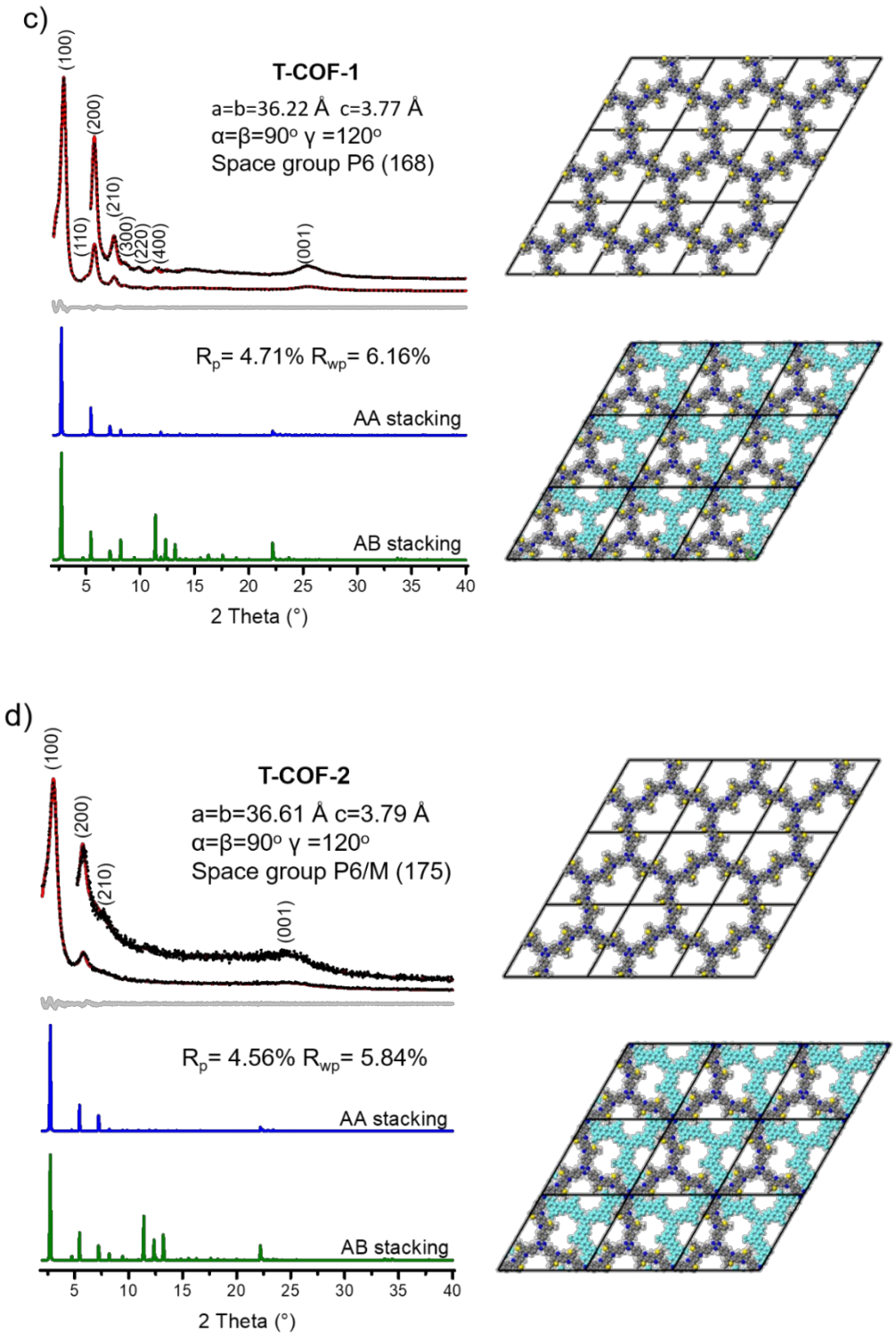

Figure S3. a) Indexed experimental (black), Pawley-refined (red) PXRD patterns with their difference(gray) and the theoretical patterns of AA stacking model (blue) and AB-stacking model (green) of **B-COF-1**. Inset: zoomed view of the detailed PXRD profile without primary peaks; for B-COF-2, T-COF-1 and T-COF-2, see (b), (c) and (d).

Table S1. Fractional atomic coordinates for the unit cell of **B-COF-1** with AA stacking.

P6 (168)							
a = b = 36.3649 Å, c = 3.8378 Å, α = β = 90°, γ = 120°							
C1	1.4071	1.56021	0.83586	C17	1.9305	1.59623	1.1563
C2	1.4284	1.60225	0.95656	C18	1.90079	1.56109	1.33558
C3	1.41095	1.62841	0.90796	C19	1.07648	1.36818	1.05197
C4	1.37221	1.6136	0.72924	H20	1.45773	1.61456	1.10133
C5	1.35193	1.57187	0.59614	H21	1.42718	1.65961	1.02544
C6	1.36892	1.54536	0.65314	H22	1.32296	1.55952	0.44605
C7	1.35231	1.64086	0.69696	H23	1.35219	1.51318	0.55383
C8	1.3775	1.68539	0.69354	H24	1.41162	1.69983	0.69784
C9	1.46896	1.89211	0.91417	H25	1.50196	1.90598	0.84055
N10	1.45427	1.9156	1.07203	H26	1.42221	1.46095	1.17004
C11	1.47722	1.95624	1.19027	H27	1.89699	1.50439	1.55009
C12	1.45614	1.47802	1.20808	H28	1.87022	1.55617	1.41905
C13	1.4777	1.45585	1.31584	H29	1.08074	1.35296	1.28685
C14	1.95498	1.54705	1.26545	H30	1.10539	1.38061	0.88771
C15	1.91502	1.53338	1.40294	H31	1.04884	1.34393	0.90221
S16	1.97626	1.59575	1.06393				

Table S2. Fractional atomic coordinates for the unit cell of **B-COF-2** with AA stacking.

P6/M (175)							
a = b = 37.0995 Å, c = 3.78 Å α = β = 90° γ = 120°							
H1	-0.08646	-0.71993	-0.22766	C15	-0.58727	-0.54699	0
C2	-0.24303	-0.63709	0	C16	-0.91617	-0.3893	0
C3	-0.2274	-0.6649	0	C17	-0.09618	-0.65271	0
C4	-0.18471	-0.65093	0	C18	-0.0629	-0.65947	0
C5	-0.1547	-0.60833	0	S19	-0.01536	-0.61567	0
C6	-0.17034	-0.58054	0	C20	-0.068	-0.70204	0
C7	-0.21289	-0.59431	0	H21	-0.24718	-0.69815	0
C8	-0.10769	-0.58986	0	H22	-0.17738	-0.675	0
N9	-0.08536	-0.54735	0	H23	-0.14969	-0.54718	0
C10	-0.04326	-0.5241	0	H24	-0.22069	-0.57004	0
C11	-0.01924	-0.54366	0	H25	-0.95651	-0.53346	0
C12	-0.97593	-0.51932	0	H26	-0.71696	-0.40809	0
C13	-0.71036	-0.34764	0	H27	-0.1267	-0.679	0
C14	-0.69521	-0.37576	0	H28	-0.0374	-0.70063	0

Table S3. Fractional atomic coordinates for the unit cell of **T-COF-1** with AA stacking.

P6 (168)							
a = b = 36.2164 Å, c = 3.7705 Å $\alpha = \beta = 90°$ $\gamma = 120°$							
C1	-0.5959	-0.4408	0.83953	C16	-0.5967	-0.6664	1.11831
C2	-0.5707	-0.3967	0.89521	C17	-0.561	-0.6613	1.29197
C3	-0.5876	-0.37	0.84053	C18	-0.533	-0.6192	1.36305
C4	-0.6302	-0.3868	0.73333	C19	-0.3674	-0.291	1.01108
C5	-0.6551	-0.4309	0.67037	H20	-0.5382	-0.3828	0.98739
C6	-0.638	-0.4576	0.72165	H21	-0.5676	-0.3362	0.89328
C7	-0.6491	-0.359	0.70627	H22	-0.6879	-0.4448	0.58488
N8	-0.6238	-0.3159	0.70714	H23	-0.658	-0.4915	0.67568
C9	-0.5301	-0.1095	0.91628	H24	-0.4965	-0.0964	0.86175
N10	-0.5452	-0.0853	1.05641	H25	-0.5782	-0.5397	1.15988
C11	-0.5226	-0.0441	1.16964	H26	-0.5558	-0.6871	1.36935
C12	-0.5441	-0.5224	1.18968	H27	-0.5036	-0.6085	1.50791
C13	-0.5222	-0.5446	1.29253	H28	-0.3797	-0.2744	0.84219
C14	-0.4531	-0.4074	1.23311	H29	-0.3431	-0.2947	0.86097
S15	-0.5963	-0.6199	1.03543	H30	-0.3521	-0.2712	1.2487

Table S4. Fractional atomic coordinates for the unit cell of **T-COF-2** with AA stacking.

P6/M (175)							
a = b = 36.6104 Å, c = 3.7907 Å $\alpha = \beta = 90°$ $\gamma = 120°$							
H1	0.91174	0.27701	-0.22744	C15	0.41148	0.45262	0
C2	0.75463	0.36192	0	C16	0.08527	0.61215	0
C3	0.76928	0.33318	0	C17	0.9021	0.34525	0
C4	0.81247	0.34709	0	C18	0.93575	0.33827	0
C5	0.84303	0.39045	0	S19	0.98399	0.38257	0
C6	0.82736	0.41894	0	C20	0.93045	0.29508	0
C7	0.78425	0.40503	0	H21	0.74725	0.29955	0
C8	0.89065	0.40906	0	H22	0.81966	0.32253	0
N9	0.91337	0.45214	0	H23	0.84831	0.45274	0
C10	0.95605	0.4756	0	H24	0.77424	0.4283	0
C11	0.98029	0.45568	0	H25	0.04401	0.46598	0
C12	0.02441	0.48039	0	H26	0.87114	0.31867	0
C13	0.29118	0.65297	0	H27	0.96142	0.29643	0
N14	0.3051	0.62484	0				

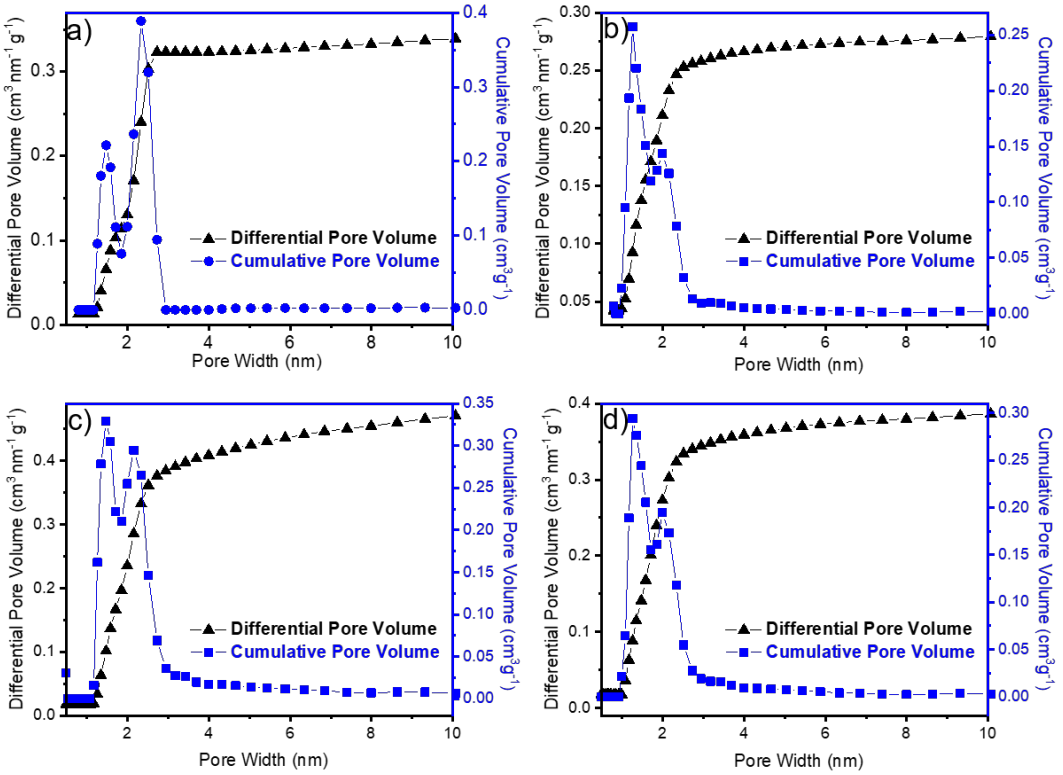

Figure S4. Pore size (blue) and pore size distribution (black) profiles of **B-COF-1** (a), **B-COF-2** (b), **T-COF-1** (c) and **T-COF-2** (d).

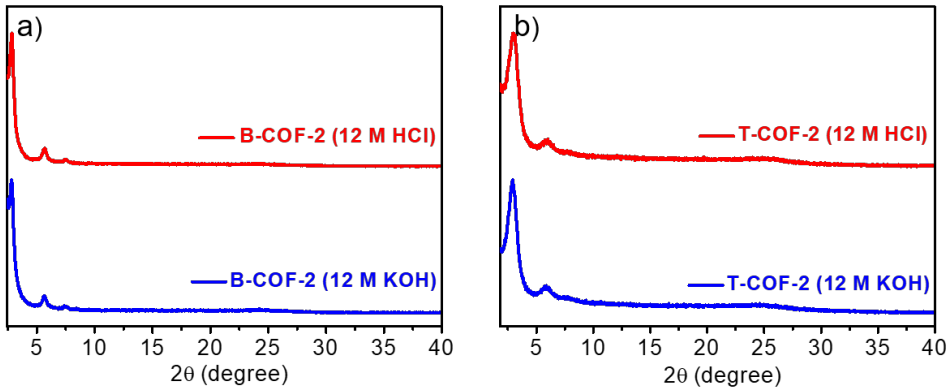

Figure S5. Chemical stability of **B-COF-2** and **T-COF-2**. PXRD patterns of **B-COF-2** (a) and **T-COF-2** (b) after treatment with 12 M HCl or 12M KOH at 50 °C for 1 day.

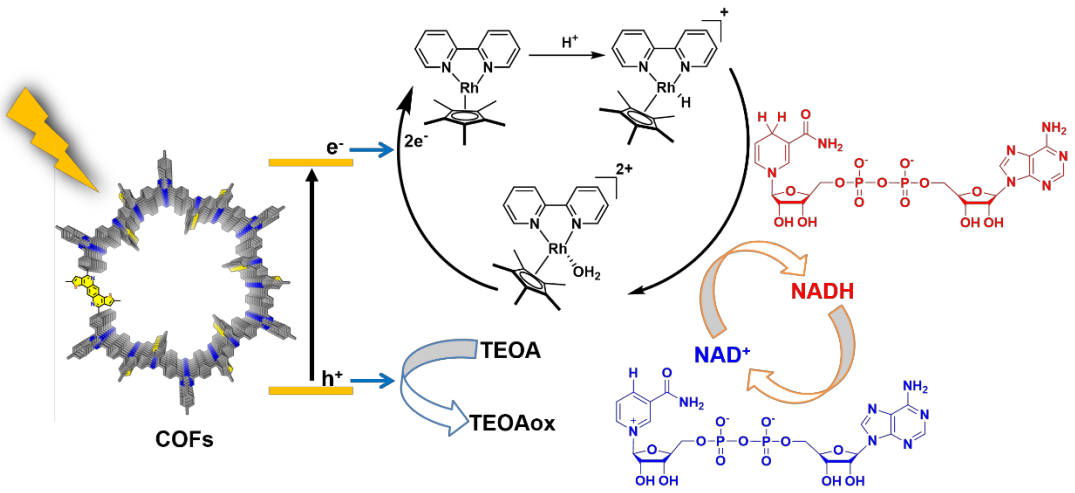

Figure S6. The process of photocatalytic NADH regeneration.

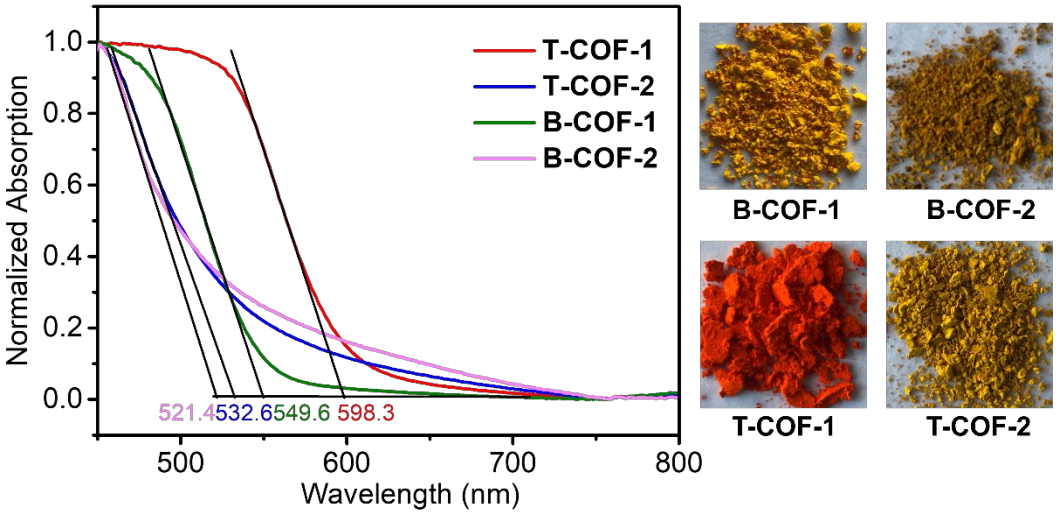

Figure S7. The solid-state absorption spectrum and digital images of **B-COF-1**, **2** and **T-COF-1**, **2**.

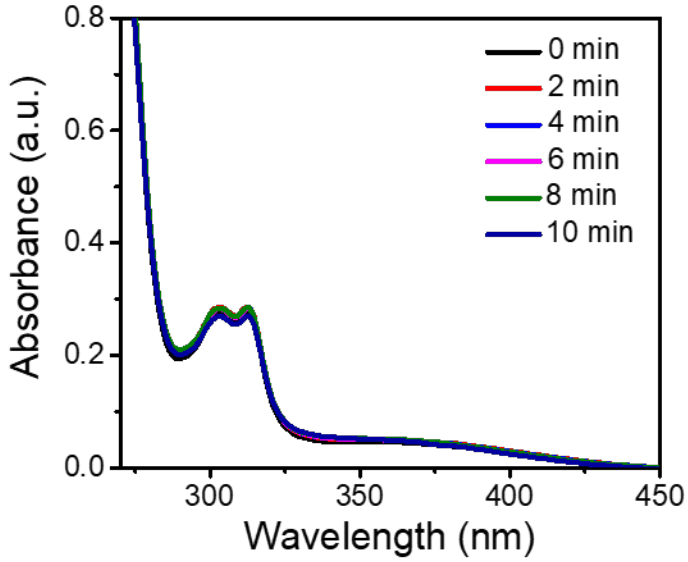

Figure S8. The experimental results of NADH regeneration without COFs, and the results showed no regeneration occurred.

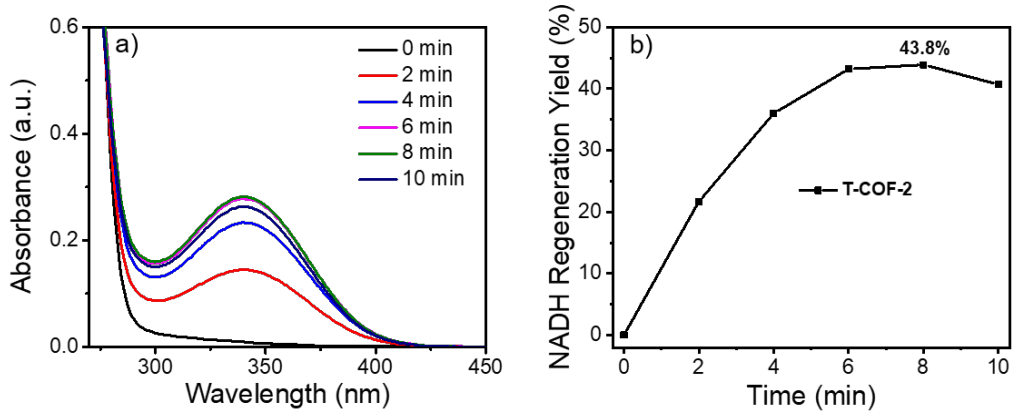

Figure S9. The experimental results of NADH regeneration without the electron mediator M: (a) absorbance changes of NADH (b) photocatalytic NADH regeneration kinetic.

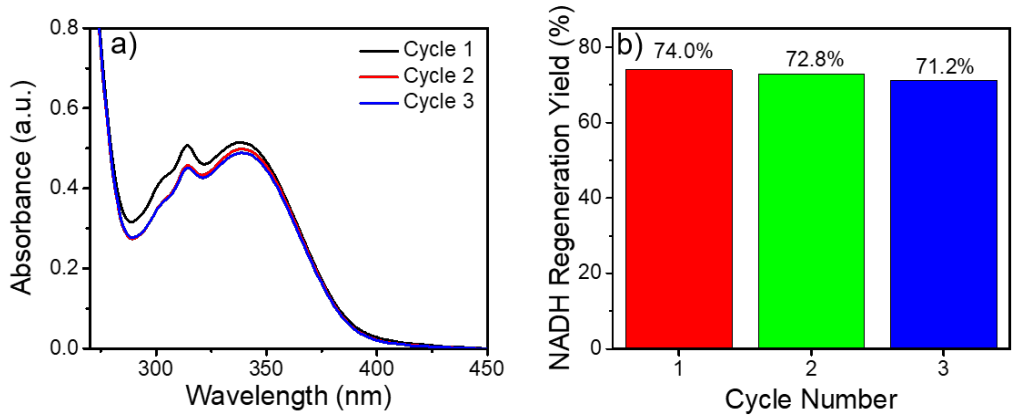

Figure S10. (a-b) Photoregeneration activity of TP-COF during repeated uses. The turnover number was 3.

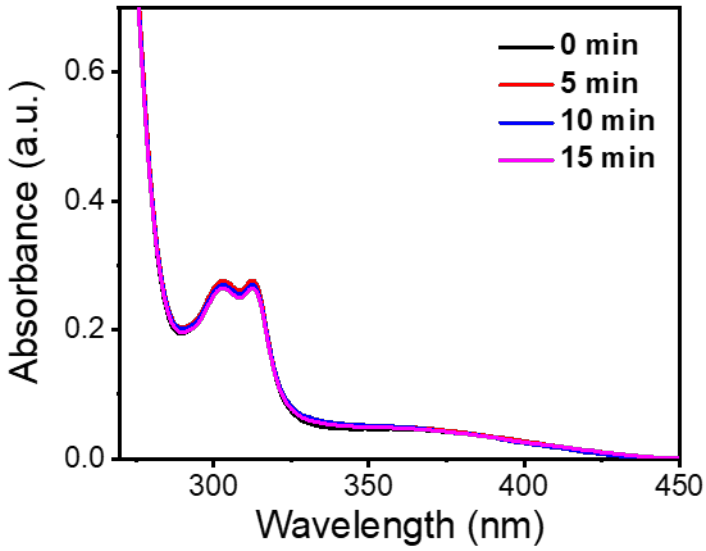

Figure S11. NADH regeneration with model compound **Ref-2**.

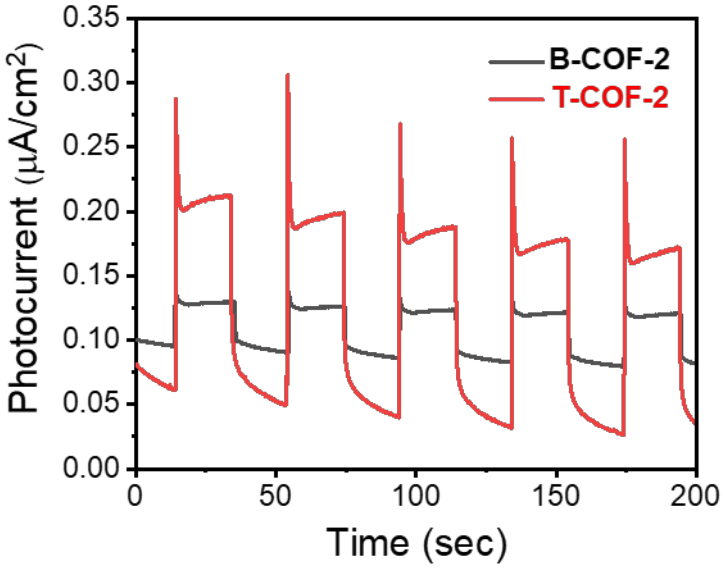

Figure S12. The photocurrent profiles of **B-COF-2** and **T-COF-2** casted on FTO glass at 0.2 V bias vs Ag/AgCl in a 0.1 M Na_2SO_4 solution.

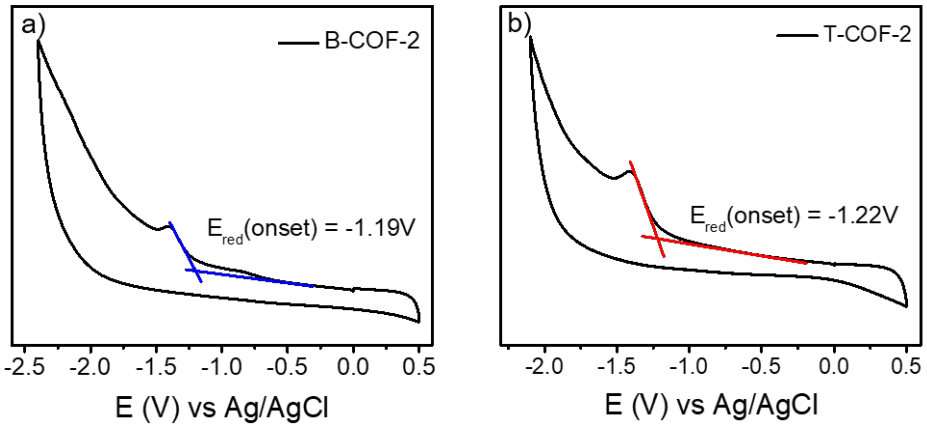

Figure S13. The CV curves of the **B-COF-2** (a) and **T-COF-2** (b) measured in acetonitrile.

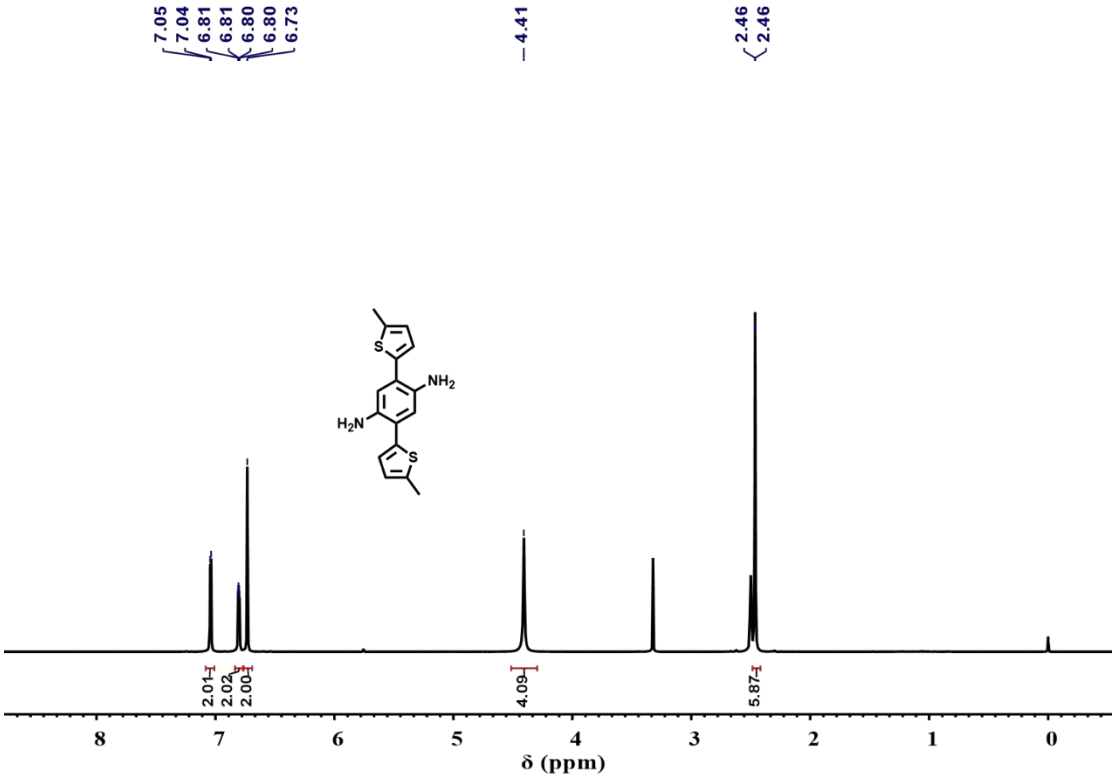

Figure S14. ^{1}H NMR spectrum of compound **A**.

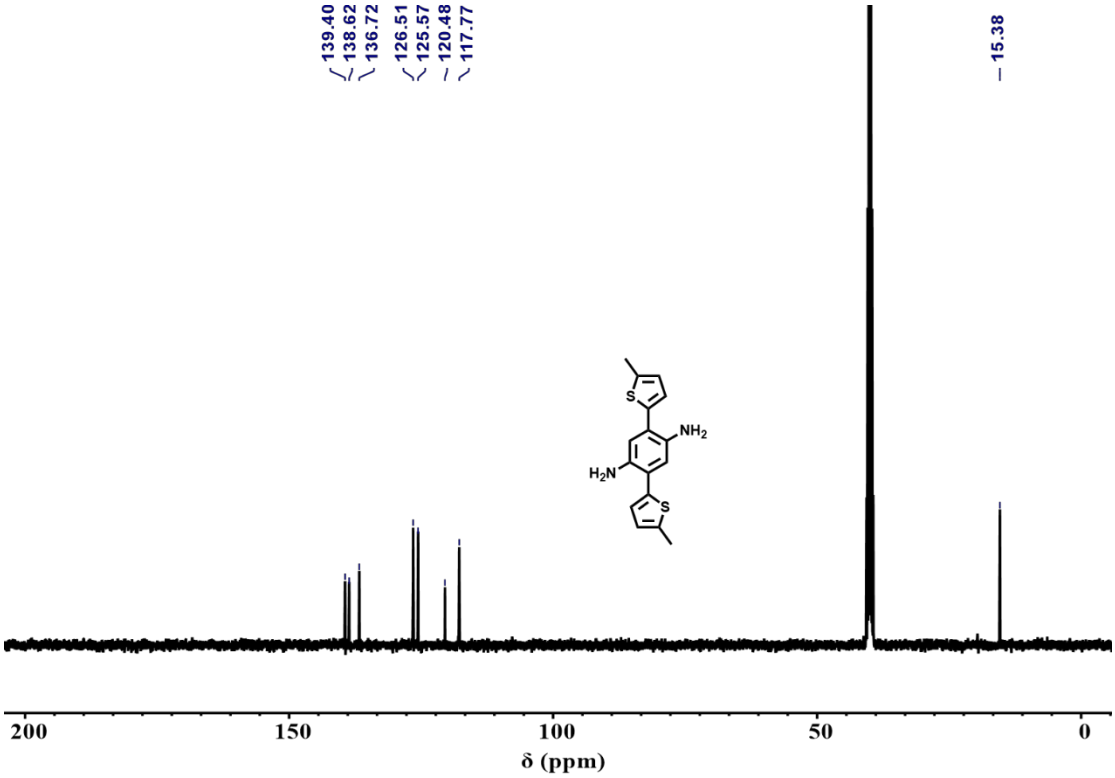

Figure S15. ^{13}C NMR spectrum of compound **A**.

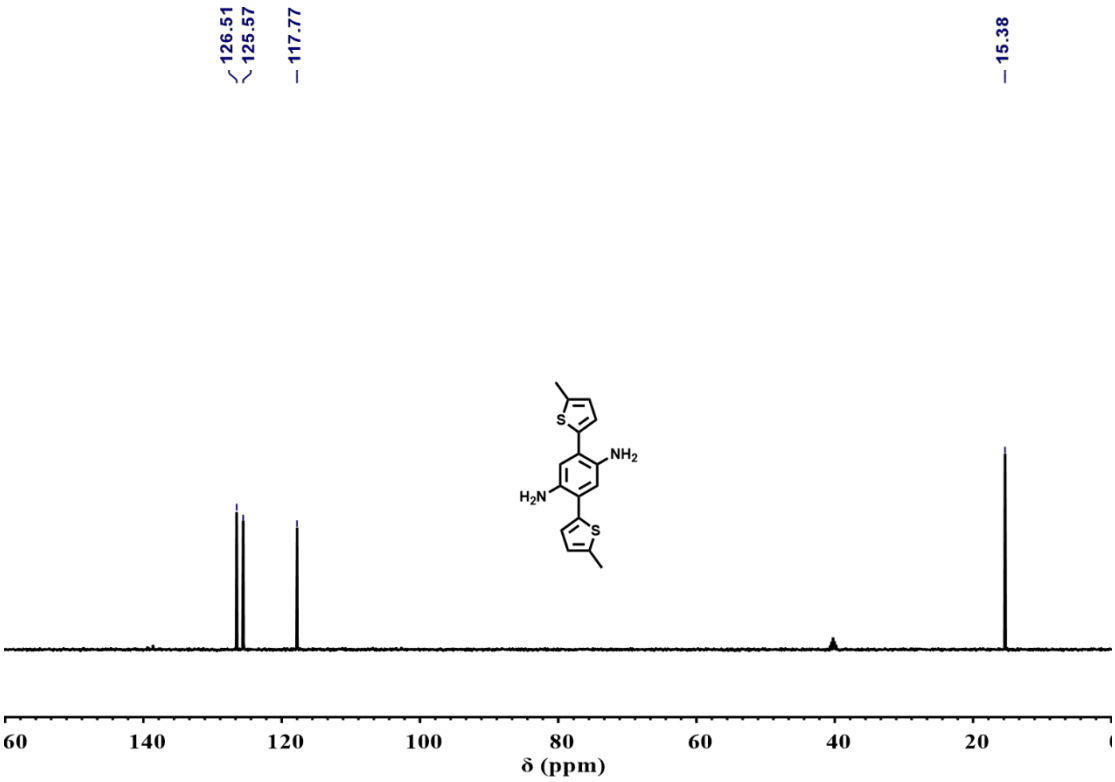

Figure S16. ^{13}C DEPT-135 spectrum of compound **A**.

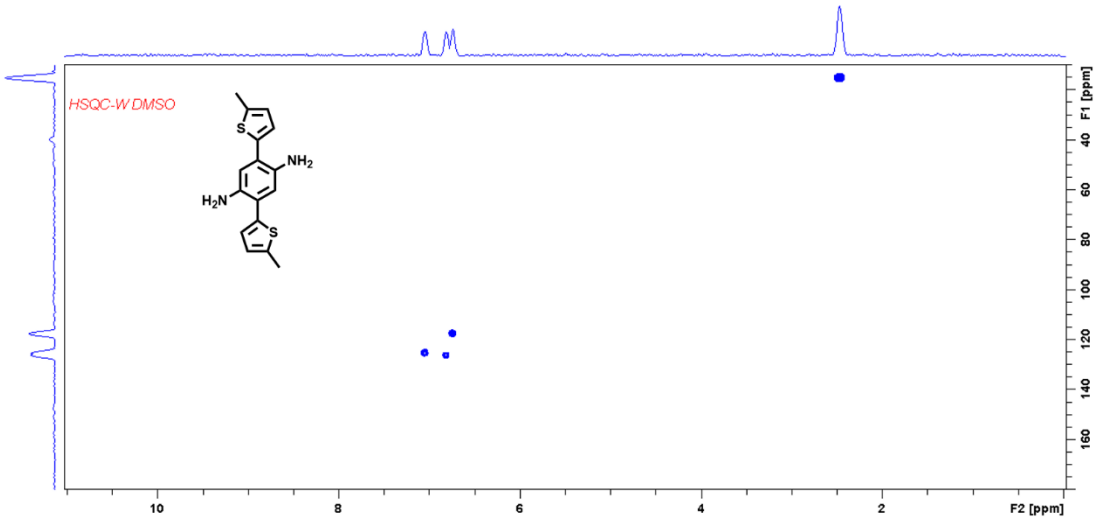

Figure S17. HSQC spectrum of compound **A**.

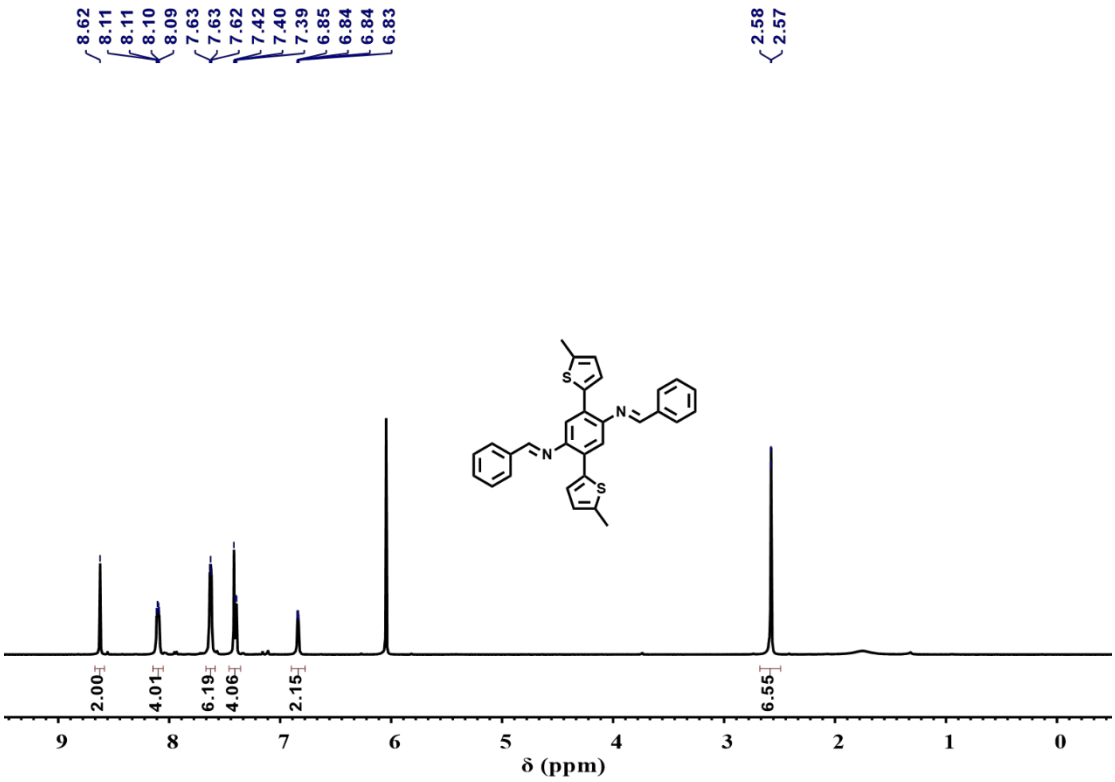

Figure S18. ^{1}H NMR spectrum of **Ref-1**.

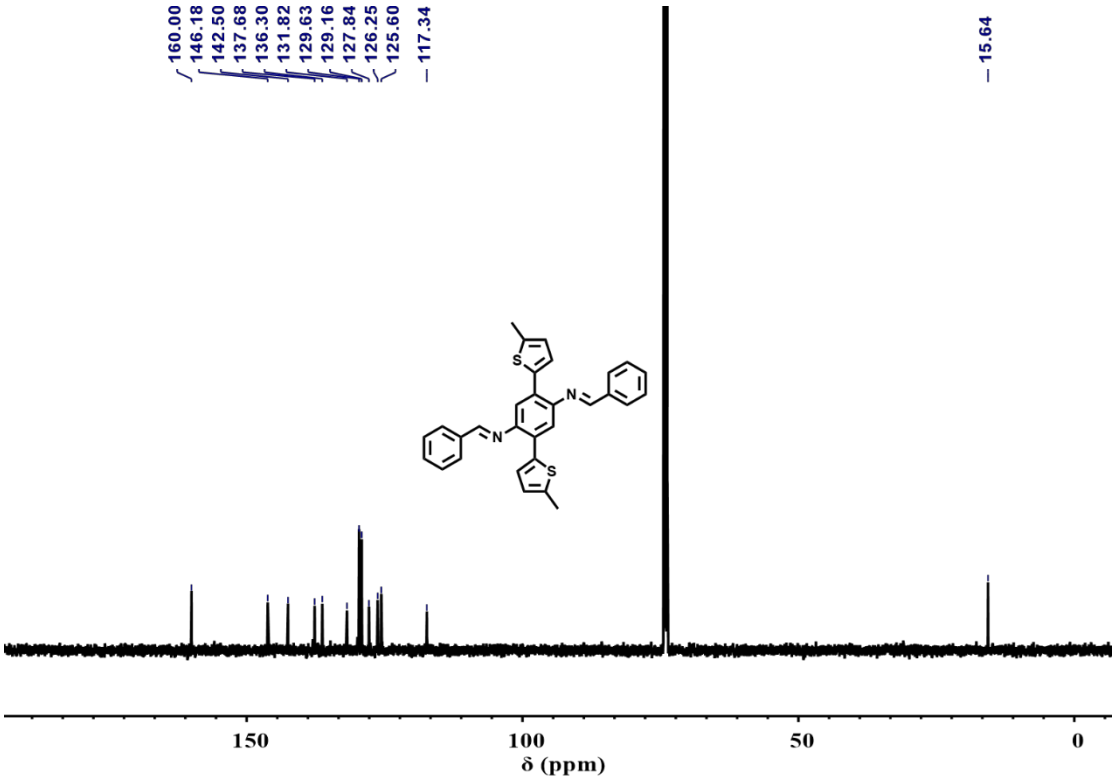

Figure S19. ^{13}C NMR spectrum of **Ref-1**.

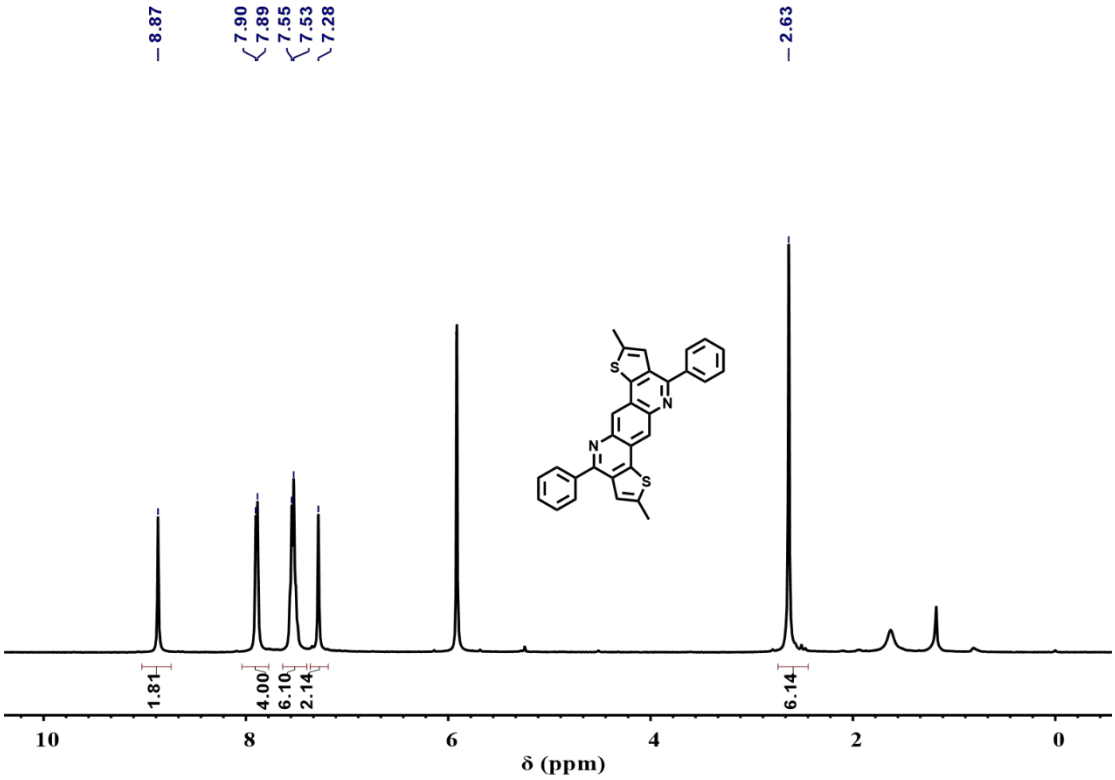

Figure S20. ^{1}H NMR spectrum of **Ref-2**.

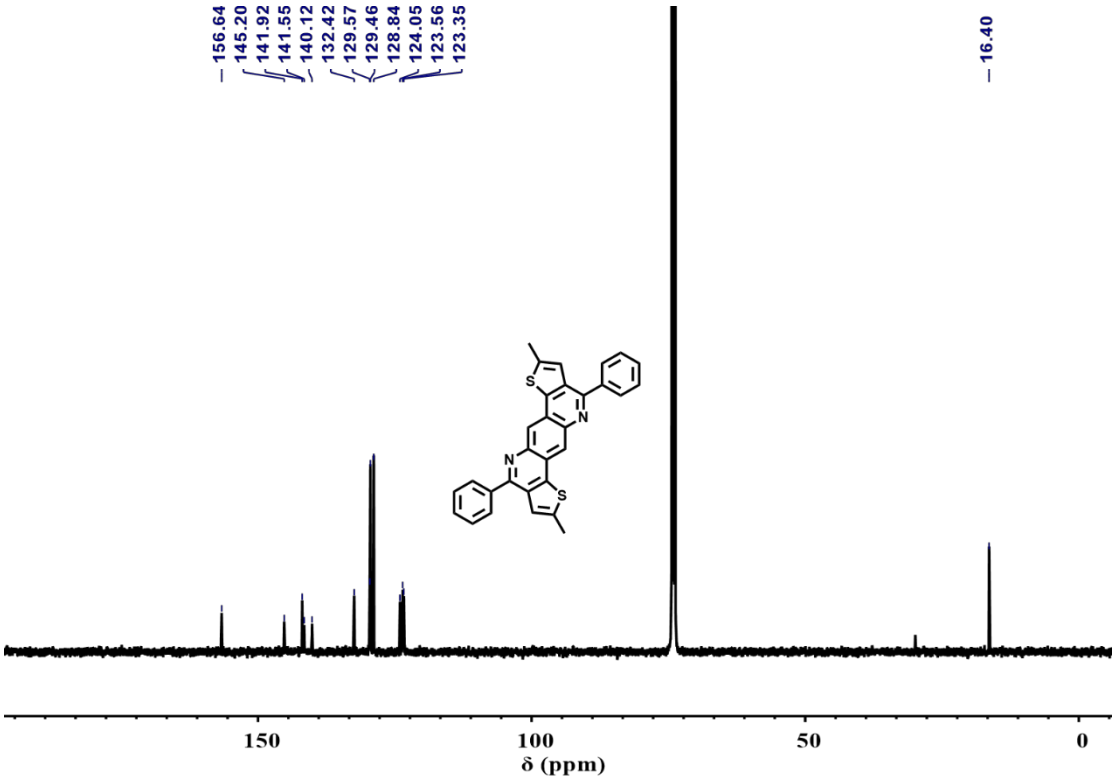

Figure S21. ^{13}C NMR spectrum of **Ref-2**.

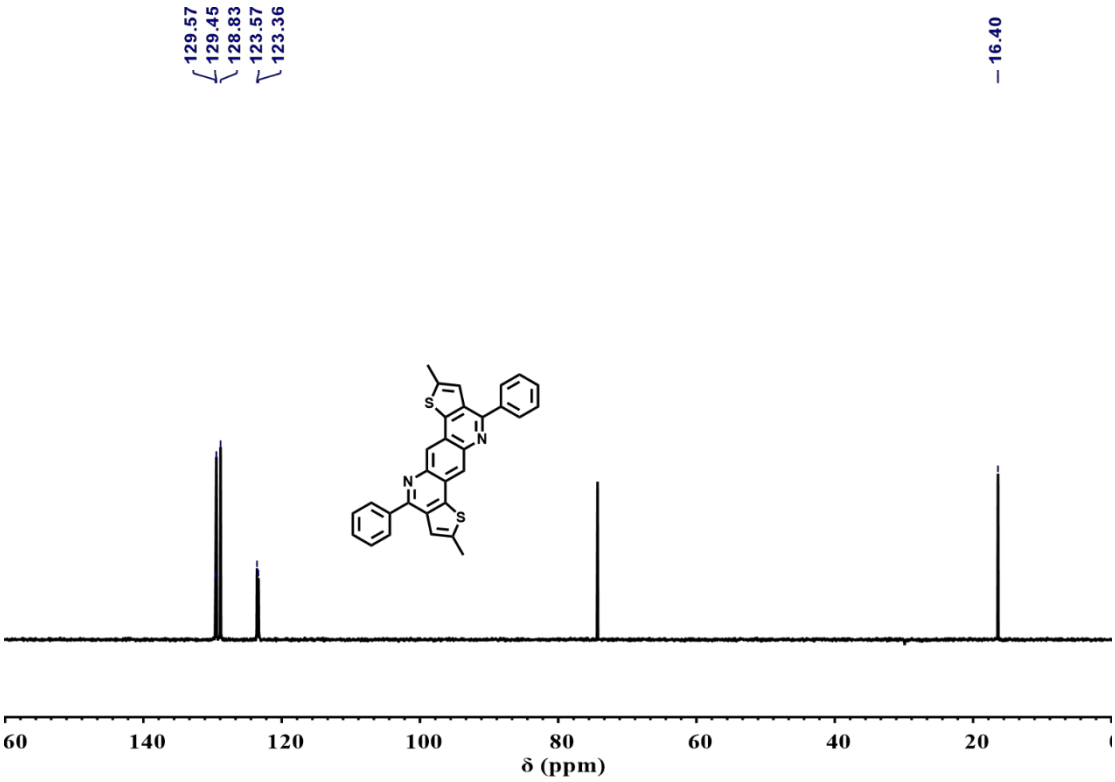

Figure S22. ^{13}C DEPT-135 spectrum of **Ref-2**.

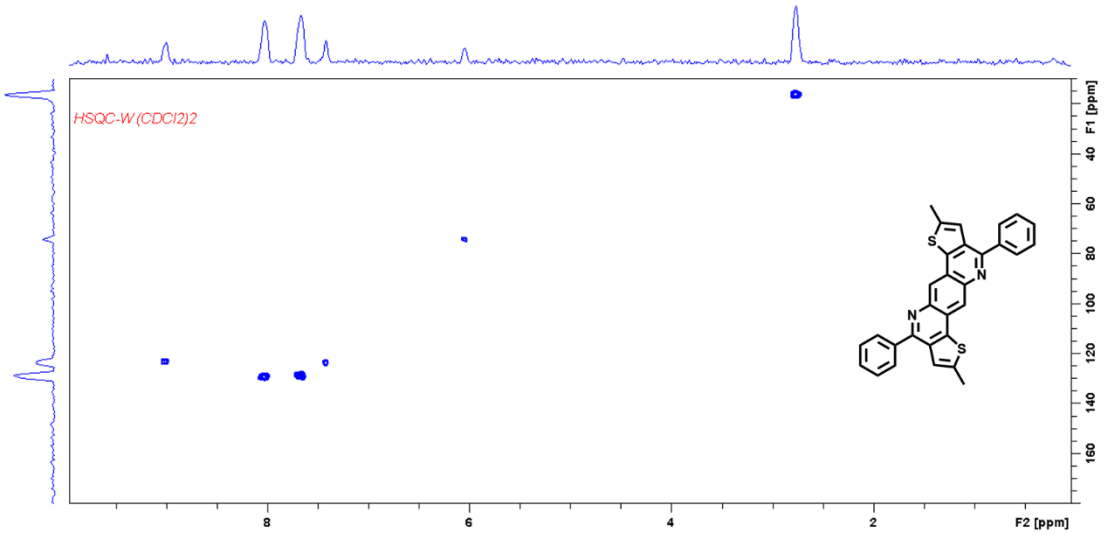

Figure S23. HSQC spectrum of spectrum of **Ref-2**.

3. References

[S1] Greenaway, R. L.; Santolini, V.; Bennison, M. J.; Alston, B. M.; Pugh, C. J.; Little, M. A.; Miklitz, M.; Eden-Rump, E. G. B.; Clowes, R.; Shakil, A.; Cuthbertson, H. J.; Armstrong, H.; Briggs, M. E.; Jelfs, K. E.; Cooper, A. I., *Nat. Commun.* **2018,** *9*, 2849.

[S2] Sekizkardes, A. K.; Altarawneh, S.; Kahveci, Z.; İslamoğlu, T.; El-Kaderi, H. M., *Macromolecules* **2014,** *47*, 8328-8334.